the new absorption coefficients determined by Farmer (*11*) for the lines listed in Table 1 (except for 8169.995 Å, which has not been measured and for which the mean value of the other lines was used), and we assumed Voigt profiles with a surface pressure of 6 mb and a temperature of 225°K (*5*); we then determined from tables the amount of precipitable water vapor in the total atmospheric path length (*12*). By assuming an effective air mass or atmospheric path length of 3, for a meridional strip of the atmosphere, we derived the amount of precipitable water in a vertical column and its mean error for each plate (Table 1). The apparent abundance values of 45 to 50 μ (0.0045 to 0.0050 g cm^{-2}) of precipitable water are larger than any determination for the whole planet during the northern spring-summer season.

Figure 2 shows these abundances determined at $L_s = 323°$ and 339° plotted on a modified version of the graph (*7*) which contains all the reliable water vapor abundance determinations as a function of L_s. All abundances have been determined by use of Farmer's improved line strengths (*11*). Also included are Antoniadi's mean regression curves for the north and south polar caps (*13*); 1969 polar regression curves are in preparation (*8*).

Figure 2 is consistent with a correlation between the behavior of the polar caps and the appearance, disappearance, and the amounts of Martian atmospheric H_2O. Although this correlation is suggestive, it does not necessarily imply a cause-and-effect relationship between the two phenomena. The data suggest that the water vapor may appear slightly later in the Martian season when the south cap is receding, rather than when the north cap is receding, and also that a slightly larger amount of H_2O may be present in the southern summer. Such effects could be consistent with expectations based on the ellipticity of the Martian orbit. Thus the south polar cap, which becomes larger than the north polar cap because it is formed during the longer, colder winter at aphelion, may have more water to release but does so at a later seasonal date. Although some water must freeze out on the caps (because the temperature of the caps is low enough and the water vapor is there at times), we feel that several processes—H_2O snow, frost, or adsorption—may well contribute to the observed behavior of the Martian H_2O at the same or at different times during the Martian seasons.

One hypothesis assumes that when water disappears from the atmosphere, a substantial part of it is trapped in the frozen carbon dioxide polar caps (*14*). As an alternative explanation (*15*), appreciable amounts of H_2O could be tied up in surface soils, which would allow the warmer southern perihelion summer to release a larger amount at that phase from the soil. Observations during additional Martian years hold out the prospect of being able to distinguish among any yearly, seasonal, or weather-caused differences in the time of appearance and amount of Martian water vapor.

EDWIN S. BARKER
McDonald Observatory, University of Texas, Fort Davis 79734
RONALD A. SCHORN
Jet Propulsion Laboratory, Pasadena, California 91103
ANDRZEJ WOSZCZYK
Torun Astronomical Observatory, Torun, Poland
ROBERT G. TULL
Department of Astronomy, University of Texas, Austin 78712
STEPHEN J. LITTLE*
McDonald Observatory, University of Texas

References and Notes

1. The term L_s is defined as the planetocentric longitude of the sun and is measured in the plane of the orbit of the planet from the ascending node on its equator. At the beginning of spring in the northern hemisphere of Mars, $L_s = 0°$.
2. Detection of a weak nonterrestrial water line is possible because of the planet's relative radial component of orbital velocity with respect to the earth; this causes a Doppler displacement, which shifts the nonterrestrial water vapor line into the outer wings of the terrestrial water vapor line where the planetary line can be detected. Such work requires spectra with high dispersion and resolution, a good Doppler shift (≧0.2 Å), and low terrestrial humidity.
3. H. Spinrad, G. Münch, L. D. Kaplan, *Astrophys. J.* **137**, 1319 1963); L. D. Kaplan, G. Münch, H. Spinrad, *ibid.* **139**, 1 (1964).
4. R. A. Schorn, H. Spinrad, R. C. Moore, H. J. Smith, L. P. Giver, *ibid.* **146**, 743 (1967).
5. R. A. Schorn, C. B. Farmer, S. J. Little, *Icarus* **11** (3), 283 (1969); T. Owen and H. P. Mason, *Science* **165**, 893 (1969); S. J. Little, in *Planetary Atmospheres Int. Astron. Union Symp. 40th*, in press.
6. R. G. Tull, *Icarus*, in press.
7. R. A. Schorn, in *Planetary Atmospheres Int. Astron. Union Symp. 40th*, in press.
8. E. S. Barker, R. A. Schorn, R. G. Tull, A. Woszczyk, S. J. Little, in preparation.
9. We express our gratitude to J. B. Oke for permission to use the California Institute of Technology microdensitometer.
10. C. E. Moore, M. G. J. Minnaert, J. Houtgast, "The Solar Spectrum 2935 Å to 8770 Å, Second Revision of Rowland's Preliminary Table of Solar Spectrum Wavelengths," *Nat. Bur. Stand. U.S. Mongr. 61* (1966).
11. C. B. Farmer, in preparation.
12. P. A. Jansson and C. L. Korb, *J. Quant. Spectros. Radiat. Transfer* **8**, 1399 (1968).
13. E. M. Antoniadi, *la Planète Mars, 1659–1929* (Herman, Paris, 1930).
14. R. B. Leighton and B. C. Murray, *Science* **153**, 136 (1966); E. S. Barker, thesis, University of Texas, Austin (1969); G. Neugebauer, G. Münch, S. C. Chase, Jr., H. Hatzenbeler, E. Miner, D. Schofield, *Science* **166**, 98 (1969).
15. J. B. Pollack, D. Pitman, B. N. Khare, C. Sagan, "Goethite on Mars: A Laboratory Study of Physically and Chemically Bound Water in Ferric Oxides," *Smithson. Astrophys. Obs. Spec. Rep.* 314 (1970).
16. Supported by grants from the National Aeronautics and Space Administration, Office of Lunar and Planetary Programs. One phase of research was carried out at the Jet Propulsion Laboratory, California Institute of Technology, under contract NAS-7-100, sponsored by NASA.
* Present address: Department of Physical Science, Ferris State College, Big Rapids, Michigan 49307.

5 August 1970; revised 13 October 1970

Molecular Microscopy: Fundamental Limitations

Abstract. *On the basis of estimates of molecular damage caused by the observation process, it is concluded that molecular microscopy of biological molecules in which the individual atoms are resolved is impossible with an electron or x-ray microscope. Microscopes that use low-energy helium atoms or neutrons as illuminants may be capable of serving as ultimate biomolecular microscopes.*

X-ray and neutron diffraction studies have served as the principal means for the determination of molecular structure. The diffraction pattern of a macroscopic crystalline sample of the molecule under investigation is analyzed to obtain information concerning the atomic arrangement in the molecules. For the giant molecules of biological interest unraveling the diffraction pattern to obtain the molecular structure is a difficult task and is sometimes ambiguous because of the phase problem (*1*). Furthermore, many biological molecules cannot be crystallized without serious structural modifications. For these and other reasons it would be very desirable to have a device, a molecular microscope, which could form an image of the individual atoms in a single molecule. With such an instrument, for example, one might be able to observe a molecule while it is undergoing a reaction, or perform an operation on a biological molecule in which a selected small group of atoms could be excised or altered.

Molecular microscopy, however, is subject to a fundamental limitation. To resolve the individual atoms of a molecule, the illuminating radiation must have a wavelength λ less than about 1

Table 1. The ionization cross section (σ_i), elastic scattering cross section (σ_e), and $R = \sigma_i/\sigma_e$ for electrons and x-rays for some atoms of biological interest (σ is in units of 10^{-16} cm^2 multiplied by the power of 10 appearing in parentheses). The electron cross sections for C and O differ from the values for N by only about 10 percent and those for P and Th differ from those for S and U, respectively, by only a few percent.

Illuminant energy (kev)	H			N			S			U		
	σ_i (Å^2)	σ_e (Å^2)	R	σ_i (Å^2)	σ_e (Å^2)	R	σ_i (Å^2)	σ_e (Å^2)	R	σ_i (Å^2)	σ_e (Å^2)	R
Electrons as illuminant												
1	1.1(−1)	2.7(−2)	4	4.7(−1)	6.3(−1)	0.75	7.7(−1)	2.5	0.3			
10	1.8(−2)	2.8(−3)	6	9.1(−2)	6.4(−2)	1.4	1.8(−1)	2.6(−1)	0.7	6.3(−1)	3.1	0.2
100	3.0(−3)	3.0(−4)	10	1.7(−2)	8.2(−3)	2.1	3.4(−2)	3.3(−2)	1.0	1.5(−1)	4.0(−1)	0.4
200	2.1(−3)	1.6(−4)	13	1.1(−2)	5.1(−3)	2.2	2.4(−2)	2.0(−2)	1.2	1.1(−1)	2.5(−1)	0.44
X-rays as illuminant												
6.2	6.5(−9)	9.9(−10)	7	3.8(−4)	8.6(−6)	44	1.1(−2)	5.8(−5)	201			
12.4	6.4(−9)	2.8(−10)	23	4.2(−5)	3.5(−6)	12	1.4(−3)	3.0(−5)	48			
124	4.7(−9)	3.0(−12)	1.6(3)	3.3(−6)	7.3(−8)	45	7.6(−6)	8.6(−7)	10			

Å, and to form an image each atom must scatter or absorb at least one quantum of the radiation (*2*). We may ignore the effects of the elastically scattered quanta on the molecular structure; but exciting and ionizing collisions will lead (with a certain probability) to molecular dissociation or rearrangement. The "image" formed will thus be a composite picture of the molecular structure over the history of the irradiation and may bear little relation to the original molecule (*3–5*). This result constitutes a fundamental limitation on molecular microscopy in which a particular type of radiation is used as the illuminant.

A first measure of the above limitation is simply the number of inelastic events per elastic interaction. An adequate estimate of this ratio may be obtained from average atomic cross sections for the relevant radiations. There is no fundamental understanding at this time of the structural changes in complex molecules that follow ionization. However, on the basis principally of extensive experimental studies of radiation, we conclude that molecular microscopy of biological molecules in which the prime atomic constituents C, N, and O are imaged is impossible if x-rays (*6*) or electrons are used as illuminants, and, with the possible exception of neutrons or epithermal He atoms, if any other illuminant is used.

In Table 1 we give values for the ionization cross section σ_i, the elastic cross section σ_e, and $R = \sigma_i/\sigma_e$ for electrons and x-rays for some atoms of biological interest. The x-ray cross sections were obtained from published experimental data and from theoretical calculations (*7*). For electrons we calculated the elastic cross sections in the Born approximation, using the analytic form factors of Burge and Smith (*8*). For the elastic cross section the expression (*9*) based on the Thomas-Fermi model of the atom

$$\sigma_e \cong 22\, Z_{eff}^{4/3}\,(h/mv)^2 \qquad (1)$$

is useful for interpolation purposes, if an effective charge, Z_{eff}, is introduced for light atoms to normalize the Thomas-Fermi results to the more exact Hartree-Fock results. The effective charge equals 0.43, 4.5, and 12.9 for H, N, and S, respectively. In Eq. 1 h is Planck's constant and m and v are the electron's mass and velocity, respectively.

For an ionization cross section we take

$$\sigma_i = -(NW)^{-1}\frac{dE}{dx}$$

where the energy loss per unit path length is given by the Bohr-Bethe-Bloch formula (*10*), which in the nonrelativistic region is

$$-\frac{dE}{dx} = N\frac{4\pi e^4}{mv^2} Z \ln\left(\frac{mv^2}{2I}\sqrt{\frac{e}{2}}\right) \qquad (2)$$

and we computed σ_i, using the Bakker and Segrè (*11*) values for the mean ionization potential I and taking $W =$ 50 ev (*12*) as an average energy loss per ionization. The e appearing in the argument of the logarithm (Eq. 2) is the base of the natural logarithms (elsewhere e stands for the electric charge); Z is the atomic number and N is the number of atoms per unit volume.

There exists a considerable body of experimental data on the dissociation of molecules following ionization (*13*) or excitation, but there is little theoretical understanding of these processes except for the simplest (diatomic, triatomic) molecules (*14*). A review of gas-phase dissociation modes following electron bombardment (*15*) shows that, when H_2O is ionized (by 100-ev electrons), about 20 percent of the ions dissociate. For NH_3 the ratio is about 40 percent, for CH_4 about 50 percent, and for C_2H_5OH about 90 percent. Except for the simplest molecules 50 to 100 percent of the ionizations lead to dissociations.

For molecules of biological interest gas analysis is not feasible or directly relevant. In solution there are additional molecular degradation modes (indirect action) due to the interactions with ions and free radicals formed by the radiation in the solvent (*16*). Alexander and Hamilton (*17*) have studied the amino acid residues constituting about 75 percent of the protein bovine serum albumin when the molecule is irradiated in the solid state by 2-Mev electrons and have found that about 2.4 of the amino acid residues were chemically changed for each 45 ev absorbed per molecule. Electron spin resonance studies (*4, 18*) generally indicate that at least one change in the molecular structure occurs as a result of each ionization.

It thus appears that σ_i gives a reasonable measure of the cross section for chemical change except for small molecules. From Table 1 we conclude that, even for an electron energy of as little as 1 kev, there will be an average of three inelastic interactions leading to structure change for every four electrons elastically scattered from C, N, and O (the prime constituents of biological matter). In this best case, forming an image of the heavy atoms in adenine (*19*), $C_5H_5N_5$, for example, requires the scattering of at least ten electrons, but after one or two scatterings a molecular rearrangement or dissociation would be expected, which would prevent observation of the original adenine (*20*). Although this does not prevent electron molecular microscopy if the observations are made sufficiently rapidly, considering the high state of ionization implied by "instantaneous" observation, the measure-

ments would have to be made within a molecular vibration time of $\approx 10^{-13}$ second, which is far beyond present capabilities. The large values of R obviously preclude x-ray molecular microscopy.

From Eqs. 1 and 2 and from Table 1 it is seen that R decreases as the electron energy is decreased, and it might seem that microscopy would become theoretically feasible for slower electrons or other charged particles. This is not true, however. For electrons a wavelength of $\lesssim 1$ Å implies that E is $\gtrsim 100$ ev, but for $E \approx 100$ ev σ_i is ≈ 1 to 2 Å^2 for the light elements (*21*), and R will be of the order of one.

Equations 1 and 2 are based on the Born approximation and apply also for (fast) protons (with minor modifications) or other charged particles (*22*). The arguments given for electrons with $E > 1$ kev apply for protons with $E > 2$ Mev. The ionization cross section increases as the proton velocity is decreased until it reaches a maximum of a few times the geometrical cross section at an energy $E \approx 20$ kev (*23*) ($v \approx v_0 = e^2/h \approx$ orbital velocity of outermost bound atomic electrons). For still lower energies the cross section for ejection of an atomic electron decreases but the cross section for the pickup of an electron maintains the value of the total ionization cross section on the order of several square angstroms down to subkilovolt energies (*23*).

We have also considered μ^- mesons (*24*) and He atoms (*25*) as possible illuminants. The preliminary results indicate that only for $E\mu^- \lesssim 50$ ev and $E_{He} \lesssim 400$ ev would their ionization cross sections be less than a few tenths of a square angstrom. Aside from the practical limitation that such slow mesons have a flight path of only 60 cm before decay, multiple scattering resulting from the large elastic atomic cross sections would make molecular microscopy difficult, if not impossible. In the case of He atoms, molecular damage from knock-on processes would limit the energy to $< \approx 10$ ev at most. At such low energies the atoms are impenetrable, but, for example, the very nondestructive He atom microscope ($E_{He} \approx 0.1$ ev) might be very useful in the transmission mode to determine the holes or channels in a molecule, and in the reflection mode to determine the positions of the surface atoms of a biological molecule.

Finally, we considered the neutron microscope. The relevant cross sections (for thermal neutrons) (Table 2) indicate that such a microscope would mainly image the H atoms, and that there would be on the order of at least one N capture event for every 40 atoms imaged by the use of thermal neutrons, or for 0.1-ev neutron the ratio would be $\approx 1/80$ (σ_{abs} is proportional to the inverse neutron velocity). The neutron capture by N is particularly damaging,

$$N^{14}(n,p)C^{14} + 626 \text{ kev}$$

resulting in a 580-kev proton and a 40-kev C^{14} recoil. Although the mean energy given to the sample per particle imaged would be much higher for neutrons than for electrons, one could, in principle, image on the order of 50 atoms with the use of neutrons before drastic structural changes occurred. However, aside from the practical difficulty of building a neutron molecular microscope (which would involve the equivalent of focusing a neutron beam to a spot of 1-Å dimension), it would be imperative that it be a dark-field, phase-contrast, or holographic microscope in order to approach our minimum condition of one quantum scattered per atom imaged. If, on the other hand, such a microscope relied on amplitude contrast to form the image, it would require a minimum of $\lambda^2/\sigma \approx 10^6$ neutrons scattered per atom imaged, thus making such molecular microscopy fundamentally impossible.

Crewe and his co-workers (*26*, p. 1340), using 30-kev electrons, have recently obtained electron microscopic images of U and Th atoms bound in molecules. According to Table 1, one ionization is expected to occur for every four to five electrons scattered by U. Crewe's U image was obtained after ≈ 400 scattering by that U atom. According to Table 1, there must have occurred ≈ 80 ionizations of the U atom during the formation of its image and about ten ionizations each for the C and O atoms irradiated. These ionizations must have produced radical structural modifications in the molecules containing the U or Th atoms. However, the U and Th images indicate that these atoms moved less than about 5 Å during the period of observation. But because of the great inertia of the U and Th atoms, this fact is not necessarily surprising. In the dissociation of a free UO molecule, for example, in which the U and O separate with kinetic energy ε, the kinetic energy imparted to the U atom is only $\approx 0.06\ \varepsilon$. Moreover, when the UO separation distance has increased by $\approx$ ½ Å beyond the equilibrium distance, to where the U–O force is negligible, the U atom will have moved only ≈ 0.03 Å. If we take for ε the rather large value of 1 ev, the U recoil energy is only ≈ 0.06 ev, which is very probably insufficient to move the U atom and its remaining covalently bonded neighbors (if any) a lattice spacing over the carbon substrate to which the molecule adheres.

The point is that there can be very severe dissociation and structural degradation involving the light molecular components without appreciable motion of the heavy atoms. This fact could be of great practical importance for the determination of base sequences with heavy atom tagging (*26, 27*), yet it would not affect the arguments set forth in this report ruling out the possibility of electron biomolecular microscopy as we have defined it.

Table 2. Neutron cross section (in barns) for thermal neutrons (*28*). The entries in column 4 should be multiplied by the power of 10 appearing in parentheses.

Atom	σ_{abs} (barns)	σ_{scat} (barns)	$\sigma_{abs}/\sigma_{scat}$
H	0.332	81	4.4(−3)
C	0.003	5.5	5.5(−4)
N	1.88	11.0	1.7(−1)
O	0.0002	4.2	4.8(−5)
Mg	0.063	3.6	1.8(−2)
P	0.2	3.1	6.5(−2)
S	0.52	1.2	4.3(−1)

J. R. Breedlove, Jr.*
G. T. Trammell
Department of Physics, Rice University, Houston, Texas 77001

References and Notes

1. D. C. Hodgkin, *Science* **150**, 979 (1965); S. Raman and J. L. Katz, in *Handbook of X-Rays*, E. F. Kaelble, Ed. (McGraw-Hill, New York, 1967), chap. 29.
2. The minimum resolvable distance in a microscope is given by the Abbé relation

$$d = 0.6\ \lambda/\sin\theta$$

where λ is the wavelength and θ is the scattering angle. In order to resolve neighboring atoms in a molecule we must have $\lambda/\sin\theta \lesssim 1$ Å. Under these conditions the individual atoms of the molecule may be considered to scatter (or absorb) nearly independently, and in the most efficient microscope possible there must be at least one quantum scattered or absorbed per atom imaged. Actually, at least two scattered quanta per atom are required to obtain its three positional coordinates [see (*3, 4*)].
3. J. R. Breedlove, Jr., and G. T. Trammell, *Bull. Amer. Phys Soc.* **14**, 622 (1969); a more detailed development and discussion of the results presented in this present paper will appear elsewhere.
4. J. R. Breedlove, Jr., thesis, Rice University (1970).
5. Molecular investigations by diffraction techniques are not subject to this limitation, for one commonly has a crystal containing on the order of 10^{18} identical molecules, each containing, say, 10^9 atoms. One then needs to scatter only a few orders of magnitude more than 10^9 quanta in order to obtain the structure; it is unlikely that any particular molecule will be struck.
6. We disregard here the technological problems

involved in constructing imaging devices that use the various radiations, but we are concerned with the question of their utility as microscopes if such devices should be constructed.
7. When feasible, these values were obtained from tables and numerical integrations. See C. M. Davisson, in *Alpha-, Beta-, and Gamma-Ray Spectroscopy*, K Siegbahn, Ed. (North-Holland, Amsterdam, 1965), vol. 1, chap. 2 and appendix 1; and C. H. MacGillavry and G. D. Rieck, Eds., *International Tables for X-Ray Crystallography* (Kynoch Press, Birmingham, England, 1962), vol. 3.
8. R. E. Burge and E. H. Smith, *Proc. Phys. Soc. London* **79**, 673 (1962).
9. L. Marton and L. I. Schiff, *J. Appl. Phys.* **12**, 759 (1941).
10. N. Bohr, *Phil. Mag.* **25**, 10 (1913); H. A. Bethe, *Ann. Phys.* **5**, 325 (1930); F. Bloch, *ibid.* **16**, 285 (1933).
11. C. J. Bakker and E. Segrè, *Phys. Rev.* **81**, 489 (1951).
→ A. M. Rauth and J. A. Simpson, *Radiat. Res.* **22**, 643 (1964).
13. After an ionization by a fast particle a molecule is left, on the average, with an electronic excitation energy of 10 to 20 ev. This is sufficient energy to break a maximum of two to five covalent bonds.
14. For a theoretical discussion of the effects of ionizing radiations on biological molecules, see E. J. Hart and R. L. Platzman, in *Mechanisms in Radiobiology*, M. Errera and A. Forssberg, Eds. (Academic Press, New York, 1961), vol. 1, p. 93.
15. J. D. Craggs and H. W. S. Massey, in *Encyclopedia of Physics*, S. Flügge, Ed. (Springer-Verlag, Berlin, 1959), vol. 37, p. 1; F. H. Field and J. L. Franklin, *Electron Impact Phenomena and the Properties of Gaseous Ions* (Academic Press, New York, 1957).
16. For a good review of the effects of radiation on biological molecules, see Z. M. Bacq and P. Alexander, *Fundamentals of Radiobiology* (Pergamon Press, Oxford, 1961).
→ P. Alexander and L. D. G. Hamilton, *Radiat. Res.* **13**, 214 (1960).
→ A. Pihl and T. Sanner *ibid.* **28**, 96 (1966);
→ K. Stratton, *ibid.* **35**, 182 (1968); K. G. Zimmer and A. Müller, in *Current Topics in Radiation Research*, M. Ebert and A. Howard, Eds. (North-Holland, Amsterdam, 1965), vol. 1, p. 1.
19. For example, see L. Pauling, *The Nature of the Chemical Bond* (Cornell Univ. Press, Ithaca, ed. 3, 1960), chap. 8, section 8.
20. We have in mind the breaking of covalent bonds and possible bonding in other configurations. Although the Frank-Rabinowich cage effect may prevent the dissociation of large fragments, H atoms or CH_3 radicals are commonly released in these reactions. In addition, R. L. Platzman and J. Franck [*Symposium on Information Theory in Biology*, H. P. Yockey *et al.*, Eds. (Pergamon Press, New York, 1958), p. 262] have stressed that following an ionization in a biological molecule there will be severe secondary structure modification due to the rupture of hydrogen bonds.
→ D. Rapp and P. Englander-Golden, *J. Chem. Phys.* **43**, 1464 (1965).
22. See N. F. Mott and H. S. W. Massey, *The Theory of Atomic Collisions* (Oxford Univ. Press, Oxford, ed. 3, 1965), chaps. 18 and 19.
23. F. J. De Heer, J. Schuter, H. Moustafa, *Physica* **32**, 1766 (19(→ J. B. H. Stedeford and J. B. Hasted, *Proc. Roy. Soc. London Ser. A Math. Phys. Sci.* **227**, 466 (1955); R. Browning and H. B. Gilbody, *J. Phys. B At. Mol. Phys.* **1**, No. 2, 11,499 (1968).
24. A. S. Wightman, *Phys. Rev.* **77**, 521 (1950).
25. H. C. Haydon and N. G. Utterback, *ibid.* **135A**, 1575 (1964); H. C. Haydon and R. C. Amme, *ibid.* **141**, 30 (1966).
26. A. V. Crewe, J. Wall, J. Langmore, *Science* **168**, 1338 (1970).
27. T. A. Welton, in *Proceedings of the Twenty-Seventh Annual Meeting of the Electron Microscopy Society of America*, C. J. Arceneaux, Ed. (Claitor's Publishing Div., Baton Rouge, 1969), p. 182; M. Beer, *ibid.*, p. 268.
28. D. J. Hughes and R. B. Schwartz, *Brookhaven Nat. Lab. Publ. No. 325* (1958).
29. Research supported in part by a National Aeronautics and Space Administration grant.
* National Defense Education Act predoctoral fellow; present address: EG&G, Los Alamos, New Mexico 87544.

13 July 1970; revised 28 August 1970

Regeneration of the Amputated Amphibian Limb: Retardation by Hemicholinium-3

Abstract. *Doses of hemicholinium-3 which partially paralyze the larval salamander profoundly retarded regeneration of the amputated hind limb. The drug also reduced the vascularity and mitotic index of the regenerating tissue. After withdrawal of the drug the rate of regeneration returned to normal. Atropine, in a daily dose of 40 milligrams per kilogram of body weight, did not retard growth. These findings suggest that in the salamander acetylcholine may mediate neurotrophic activity.*

Regeneration of the amputated amphibian limb requires the presence of nerve (*1*). If the nerve is transected after growth has begun, the regenerate gradually breaks down in a distoproximal direction and is resorbed (*2*). Both sensory and motor fibers can initiate and maintain limb regeneration, although in the case of the sensory nerve, the trophic influence is opposite in direction to transmission of impulses from the periphery. Drachman (*3*) has presented convincing evidence that development of striated muscle depends upon release of acetylcholine. He showed that botulinum toxin, hemicholinium-3, and curare prevented development of striated muscle in the growing chick embryo. Fat replaced the muscle mass, a condition usually seen after long-term denervation. The myocardium was unaffected.

Our interest in acetylcholine as a possible trophic factor arose from studies of children with familial dysautonomia. This disorder is characterized by a parasympathetic defect with sensory impairment and subnormal growth (*4*). Since this disorder is probably caused by a single enzyme defect (*5*), the deficiencies ought to be related. We therefore undertook a study of the effects of prolonged cholinergic blockade on tissue of gilled salamanders. The aquatic form of these salamanders was selected because respiration through the gills requires little or no muscle activity.

Ambystoma tigrinum larvae (Lemberger) weighing approximately 15 to 20 g were used in all experiments. Each animal was maintained in a separate vessel (7 by 10 by 4 inches) at room temperature. Water was changed daily. Control groups and treated groups were studied concurrently. Each week the growth rate was determined from measurement of the distance from the point of amputation (knee) to the end of the stump or the tip of the distal phalange. Phalanges did not appear until after the 5th week. The drugs were prepared in modified Ringer (amphibian) solution and injected intraperitoneally with a 25-gauge needle in volumes up to 0.5 ml. Hemicholinium-3 was injected daily or every 2nd or 3rd day, depending on the persistence of paresis.

The mean rate of limb regeneration in seven salamanders treated with hemicholinium-3 in a dose of 1.5 mg/kg was 40 ± 6 percent of the control rate (100 ± 8 percent); in seven salamanders treated with a dose of 3 mg/kg the rate of regeneration was only 34 ± 1.6 percent of the control rate (Fig. 1). These figures represent mean growth measured after 10 weeks. Growth rates during the undifferentiated stump stage and the phalangeal stage were retarded by treatment. As compared with controls, four salamanders treated with atropine in a daily dose of 40 mg/kg showed no decrease in growth rate of the regenerate.

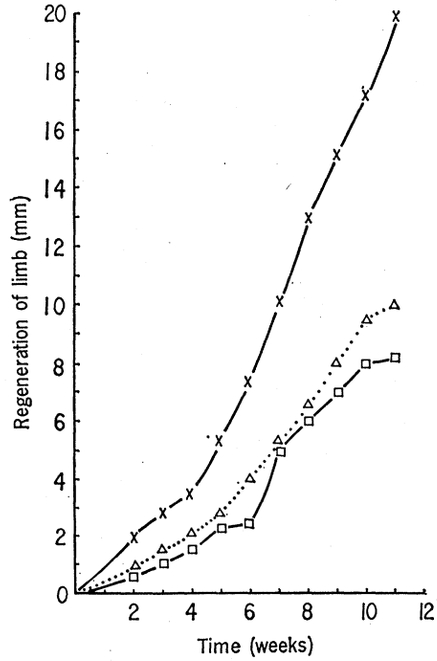

Fig. 1. Effect of injection of hemicholinium on mean growth rates of regenerating salamander limbs. Control, X; hemicholinium (1.5 mg/kg), triangles; hemicholinium (3 mg/kg), squares.